FOREX Publication
Open Access | Rapid and quality publishing

International Journal of
Electrical and Electronics Research (IJEER)
Research Article | Volume 13, Issue 1 | Pages 69-79 | e-ISSN: 2347-470X

PI Backstepping Control of a Surface-Mounted Permanent Magnet Synchronous Motors

Sros Nhek[1*], Sarot Srang[2], Channareth Srun[3], Chivon Choeung[4,a], and Horchhong Cheng[4,b]

[1]*Graduate School, National Polytechnic Institute of Cambodia, Phnom Penh, Cambodia; Email: nheksros@npic.edu.kh*
[2]*Industrial and Mechanical Engineering, Institute of Technology of Cambodia, Phnom Penh, Cambodia; Email: srangsarot@itc.edu.kh*
[3]*Faculty of Electronic, National Polytechnic Institute of Cambodia, Phnom Penh, Cambodia; Email: nareth16npic@gmail.com*
[4]*Faculty of Electricity, National Polytechnic Institute of Cambodia, Phnom Penh, Cambodia; Email: choeungchivon@npic.edu.kh[a], horchhong@gmail.com[b]*

***Correspondence:** Sros Nhek; *nheksros@npic.edu.kh*

ABSTRACT- Backstepping control is a systematic technique for stabilizing nonlinear systems, particularly Permanent Magnet Synchronous Motors (PMSMs), by addressing their coupled electrical and mechanical dynamics. This Lyapunov-based approach allows for the design of control laws in a step-by-step manner, enhancing stability and performance under uncertainties. This paper presents a comprehensive evaluation of the PI Backstepping (PI-BS) Controller for speed regulation of PMSMs, showing significant improvements in dynamic performance, stability, and disturbance rejection compared to the Gain-Scheduled PI (GSPI) Controller. The control design focuses on rotor speed regulation through q-axis current, ensuring global asymptotic stability via Lyapunov criteria. Simulation results demonstrate the PI-BS controller's superior performance: during a step change from 0.2 PU to 0.9 PU, it achieves a rise time of 19.26ms and minimal overshoot of 0.50%, outperforming the GSPI controller's 22.83ms rise time and 1.53% overshoot. Under nonlinear load disturbances at 1.0 second, the PI-BS controller recovers faster with fewer oscillations, and in a speed reversal from 0.9 PU to -0.8 PU, it outperforms the GSPI controller with a fall time of 17.92ms and an overshoot of 0.50%. By decoupling the electrical and mechanical subsystems, the PI-BS controller offers precise speed and torque regulation under varying conditions. Its Lyapunov-based stability analysis ensures global asymptotic stability, enhancing robustness against disturbances and parameter variations. The controller's faster response times, reduced overshoot, and improved disturbance rejection make it a highly reliable solution for high-performance motor control, particularly in industrial and automotive applications.

Keywords: Backstepping Control; Speed Control; Nonlinear Control.

ARTICLE INFORMATION

Author(s): Sros Nhek, Sarot Srang, Channareth Srun, Chivon Choeung, and Horchhong Cheng;
Received: 25/10/2024; **Accepted**: 15/01/2025; **Published**: 30/03/2025;
e-ISSN: 2347-470X;
Paper Id: IJEER 2510-24;
Citation: 10.37391/ijeer.130111
Webpage-link:
https://ijeer.forexjournal.co.in/archive/volume-13/ijeer-130111.html

crossref member
CROSSREF.ORG
THE CITATION LINKING BACKBONE

Publisher's Note: FOREX Publication stays neutral with regard to Jurisdictional claims in Published maps and institutional affiliations.

1. INTRODUCTION

Permanent Magnet Synchronous Motors (PMSMs) are widely utilized in industries such as automotive, aerospace, and robotics due to their high efficiency, compact size, and excellent torque-to-inertia ratio. Precise control of PMSM speed is critical in these applications, where reliability, accuracy, and robustness are essential. However, controlling PMSMs is challenging due to their nonlinear dynamics and sensitivity to parameter variations and external disturbances, which render traditional control strategies like Proportional-Integral-Derivative (PID) controllers inadequate for maintaining high performance across all operating conditions [1,2]. Although advanced control strategies such as Field-Oriented Control (FOC), Direct Torque Control (DTC), and Sliding Mode Control (SMC) have been developed to improve robustness and accuracy, they still exhibit limitations, particularly in disturbance rejection and managing parameter uncertainties [3,4].

Despite their prevalence, PID controllers struggle with the nonlinearities and parameter variations typical of PMSM systems [5,6]. Recent advancements in gain scheduling techniques aim to enhance PID performance by adjusting control parameters based on operating conditions. However, the linear nature of PID makes it unsuitable for highly nonlinear systems under varying loads and disturbances [7-10]. DTC, known for its fast dynamic response, offers torque and flux control without a decoupling network but suffers from inherent torque ripple and parameter sensitivity, limiting its application in high-precision contexts [11,12]. However, DTC's drawback is the inherent torque ripple and parameter sensitivity, which makes it less desirable in high-precision applications Additionally, both FOC and DTC can be less effective in handling large disturbances, motivating the development of more robust control strategies. [13-15]. Recent advancements in Sliding Mode Control (SMC) demonstrate enhanced robustness and reduced chattering effects in electric drive systems, with approaches such as integrating extended state observers, adaptive control strategies, boundary layers for high-speed applications, and disturbance observers, significantly improving performance under uncertainties and external disturbances [16]. By driving the system states to a sliding surface, SMC ensures that the system dynamics are insensitive to parameter variations and external disturbances [17,18]. However, the well-known drawback of SMC is the chattering phenomenon, which can lead to mechanical wear and tear of the motor and cause undesirable vibrations. While SMC provides high robustness, the chattering issue limits its application in sensitive control environments, such as high-speed PMSM systems [19].

Active Disturbance Rejection Control (ADRC) has emerged as a robust strategy for real-time disturbance estimation and compensation, handling parameter uncertainties effectively [20,21]. However, its reliance on accurate disturbance estimation and complexity can challenge its implementation in high-speed applications [22,23]. Robust control methods like H-Infinity and Mu Synthesis address uncertainties but involve complex formulations and high computational demands, hindering real-time application [24,25]. In contrast, Reinforcement Learning (RL) shows promise in learning optimal control policies through environmental interactions, outperforming traditional methods in nonlinear systems, though it requires extensive training data and is computationally intensive [26,27]. The study evaluated the performance of backstepping control in comparison to Field-Oriented Control (FOC) and Direct Torque Control (DTC). The findings revealed that, although FOC and DTC performed effectively under steady-state conditions, backstepping control demonstrated superior transient performance and disturbance rejection capabilities [28,29]. Moreover, backstepping control's design simplicity made it easier to implement in real-time compared to robust control methods like H-Infinity and Mu Synthesis [30,31]. By systematically addressing nonlinearities and ensuring global asymptotic stability, backstepping control emerges as a robust solution for PMSM speed regulation and stability, with potential for integration with adaptive control mechanisms to further enhance performance in practical applications.

Backstepping control is an effective and systematic technique for stabilizing nonlinear systems, particularly Permanent Magnet Synchronous Motors (PMSMs), by addressing their coupled electrical and mechanical dynamics. This recursive, Lyapunov-based approach allows for the design of control laws in a step-by-step manner, enhancing stability and performance in the presence of uncertainties. The control design begins with establishing a mathematical model in the d-q reference frame, focusing on controlling rotor speed through the q-axis current while ensuring global asymptotic stability via Lyapunov criteria. The process consists of two main loops: the speed control loop, which generates a torque command based on speed error, and the current control loop, which regulates the q-axis current. By constructing Lyapunov functions for both loops, backstepping ensures stability and effectively mitigates disturbances, making it a robust strategy for speed regulation in PMSMs. This paper makes significant contributions to control system design for Permanent Magnet Synchronous Motors (PMSMs) by applying a systematic backstepping control strategy to their nonlinear dynamics. The first contribution is the detailed application of backstepping, which decouples the electrical and mechanical subsystems, allowing for precise regulation of speed and torque even under varying operating conditions. This approach offers a substantial improvement over traditional linear control methods that often struggle with nonlinearities. The second key contribution involves the use of Lyapunov-based stability analysis in the speed and current control loops, ensuring global asymptotic stability (GAS). By establishing separate Lyapunov functions for each subsystem, the paper guarantees convergence of tracking errors to zero, thus enhancing system robustness against disturbances and parameter variations. Finally, the focus on efficiency and robustness allows the PMSM to handle load variations without compromising performance, making it particularly relevant for applications like electric vehicles and robotics. Overall, this paper provides both theoretical insights and practical solutions for high-performance PMSM control.

2. Mathematical Modeling of the SM-PMSM

The first step in Backstepping control design is to develop an accurate mathematical model of the PMSM. The dynamic equations of a PMSM in the *dq*-frame (rotor reference frame) are given by

2.1. Electrical Dynamics

$$V_d = R_s i_d + L_d \frac{di_d}{dt} - \omega_r L_q i_q + E_d \tag{1}$$

$$V_q = R_s i_q + L_q \frac{di_q}{dt} + \omega_r L_d i_d + E_q \tag{2}$$

where V_d, V_q are the dq-direct and quadrature axis voltages, i_d, i_q are the direct and quadrature-axis currents, R_s is the stator resistance, L_d , L_q are the dq -axis inductances, ω_r is the electrical angular velocity, P is the number of rotor permanent magnet pole pairs, λ_f is the permanent magnet flux linkage, E_d, E_q are the back EMF (electromotive force) components, which for a surface-mounted PMSM are:

$$E_d = 0 \tag{3}$$

$$E_q = \omega_r \lambda_f \tag{4}$$

2.2. Mechanical Dynamics

The mechanical dynamics of the motor are described by the motion equation Newton's second law for rotation:

$$J\frac{d\omega_r}{dt} + B\omega_r = T_e - T_l \tag{5}$$

where J is the moment of inertia, ω_r is the rotor speed, T_e is electromagnetic torque, T_l is the load torque, B is the viscous friction coefficient. The electromagnetic torque T_e of a Permanent Magnet Synchronous Motor (PMSM) can be derived from the motor's d-q axis equivalent circuit model. The torque is produced by the interaction between the stator currents and

FOREX Publication
Open Access | Rapid and quality publishing
International Journal of
Electrical and Electronics Research (IJEER)
Research Article | Volume 13, Issue 1 | Pages 69-79 | e-ISSN: 2347-470X

the rotor's magnetic field. The expression for the electromagnetic torque T_e is given by:

$$T_e = \frac{3}{2}P\left(\lambda_f i_q + \left(L_d - L_q\right)i_d i_q\right) \quad (6)$$

For surface-mounted permanent magnet synchronous motors (PMSMs), where the rotor magnets are located on the surface of the rotor and the inductances along the *d*-axis and *q*-axis are roughly identical, the torque equation can be simplified to:

$$T_e = \frac{3}{2}P\lambda_f i_q \quad (7)$$

The relationship between the angular velocity ω_r and the angular position θ_r of the rotor is given by:

$$\omega_r = \frac{d\theta_r}{dt} \quad (8)$$

3. BACKSTEPPING CONTROL DESIGN

Backstepping is a systematic control method ideal for nonlinear systems like Permanent Magnet Synchronous Motors (PMSMs), which have coupled electrical and mechanical dynamics. It decomposes the control problem into manageable steps, beginning with rotor speed control and extending to current regulation, ensuring global stability and performance.
The design starts with the PMSM's *d-q* frame model, where rotor speed is influenced by the q-axis current, and stator currents are governed by applied voltages. A Lyapunov-based criterion is employed to ensure stability at each stage. Control design proceeds in two loops (show in *figure 1*): the speed control loop minimizes the speed error to generate a torque command, while the current control loop regulates q-axis current to achieve the desired torque. By constructing Lyapunov functions for both loops, backstepping ensures error minimization and global stability.

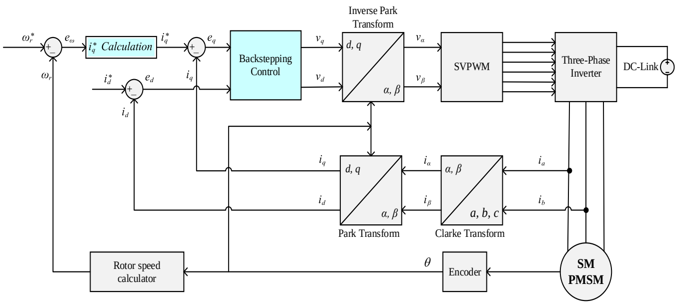

Figure 1. Diagrammatic illustration of the PI Backstepping Control structure

The control design process presented in this study emphasizes a structured approach to achieve global asymptotic stability in the speed and current control loops of a surface-mounted Permanent Magnet Synchronous Motor (PMSM). The following steps illustrate the methodological framework:

Step 1: Speed Error Calculation and Integral Term Computation
The speed error is calculated as the difference between the reference speed and the actual rotor speed. An integral term is introduced to eliminate steady-state errors and enhance robustness against disturbances. This step lays the foundation for subsequent Lyapunov-based design by defining the first tracking error dynamics.

Step 2: Lyapunov Function Selection and Derivation of the Time Derivative
A candidate Lyapunov function is carefully chosen to reflect the system's energy-like properties. Its time derivative is derived to provide insight into the system's stability. The derivative is expressed in terms of the error dynamics, which guides the design of stabilizing control laws in the following steps.

Step 3: Design of the Virtual Control Input for Speed Control
Using the Lyapunov-based approach, a virtual control input is designed to regulate the rotor speed error. The control law ensures that the derivative of the Lyapunov function is negative semi-definite, guaranteeing stability at this level. This step integrates proportional-integral action to improve tracking performance.

Step 4: Implementation of Electromagnetic Torque Control
The virtual control input is translated into a physical control action by designing an appropriate electromagnetic torque reference. This ensures that the desired torque is achieved, facilitating precise speed control while accommodating system constraints and dynamics.

Step 5: Extension of the Lyapunov Function to Stabilize Current Loops
The Lyapunov function is extended to include the dynamics of the direct and quadrature axis currents (i_dand i_q). Stabilizing control laws for current loops are derived to ensure proper electromagnetic interaction, which is critical for achieving overall system stability.

***Step 6*: Proof of Global Asymptotic Stability**
A comprehensive stability analysis is performed to establish global asymptotic stability of the overall system. The proof is based on the extended Lyapunov function and verifies that all error trajectories converge to zero. This step provides theoretical assurance of the controller's performance under varying operating conditions.

Here's a detailed breakdown of the design process for the speed control loop.

Step 1: Define the Speed Tracking Error
The speed tracking error, e_ω, is defined as the difference between the desired reference speed ω_r^* and the actual rotor speed ω_r. The goal of the speed control loop is to minimize this error, ensuring that the motor speed ω_r closely follows the desired reference speed ω_r^*.

$$e_\omega = \omega_r^* - \omega_r \quad (9)$$

where ω_r^* is the reference speed and ω_r is the actual rotor speed. We also define an integral term ξ eliminate steady-state errors:

$$\xi = \int e_\omega \, dt \quad (10)$$

Step 2: Lyapunov Function Candidate for Speed Control

A Lyapunov function is chosen to ensure the stability of the speed tracking error. We choose the following Lyapunov function that incorporates both the speed tracking error e_ω and its integral ξ.

$$V_1 = \frac{1}{2}e_\omega^2 + \frac{1}{2}k_i\xi^2 \quad (11)$$

where $k_i > 0$ is the integral gain. Since both terms are squared, $V_1 \geq 0$ or all values of e_ω and ξ, and $V_1 = 0$ only when both $e_\omega = 0$ and $\xi = 0$. Therefore, V_1 is positive definite, meaning that it reflects the energy stored in the system, and zero when the system is in equilibrium.

The time derivative of the Lyapunov function of V_1 is computed to examine how the system evolves over time. Differentiating V_1 with respect to time:

$$\dot{V}_1 = e_\omega \dot{e_\omega} + k_i\xi\dot{\xi} = e_\omega \dot{e_\omega} + k_i\xi e_\omega \quad (12)$$

The term $e_\omega \dot{e_\omega}$ represents the change in the speed tracking error with respect to time. It captures how fast the error e_ω is changing. The derivative $\dot{e_\omega}(t)$ tells us if the error is increasing or decreasing. If $\dot{e_\omega}(t) > 0$, the error is increasing, meaning the actual speed is diverging from the desired speed. If $\dot{e_\omega}(t) < 0$, the error is decreasing, meaning the system is converging towards the desired speed. The second term $k_i\xi e_\omega$ represents the contribution of the integral action in the control system. Since ξ is the integral of the speed error, its time derivative $\dot{\xi}$ is simply e_ω. The integral of the error ξ works together with the error e_ω to influence the control system, adjusting the speed to track the desired reference more accurately over time. Thus, the time derivative of the Lyapunov function $\dot{V}_1$ depends on both the current error e_ω and its rate of change $\dot{e_\omega}$, as well as the integral term ξ.

To proceed with the proof, $\dot{e_\omega}$ computes by utilizing the mechanical dynamics equation of the rotor, which captures the relationship between torque, inertia, and angular acceleration. When designing a controller to regulate the speed of a permanent magnet synchronous motor (PMSM), it is essential to consider the dynamics of the speed tracking error. Specifically, the time derivative of the speed error e_ω plays a critical role in the control design, as it directly influences the system's ability to track the desired speed and maintain stability. Understanding these dynamics helps refine the control strategy for precise and efficient motor operation.

$$\dot{e_\omega} = \frac{d}{dt}(\omega_r^* - \omega_r) = \dot{\omega}_r^* - \dot{\omega}_r \quad (13)$$

where the $\dot{\omega}_r^*$ term represents the time derivative of the reference speed and how the desired speed is changing over time. It reflects the desired acceleration or deceleration commanded by the control system. The $\dot{\omega}_r$ term represents the time derivative of the actual rotor speed, the actual acceleration or deceleration of the rotor. It reflects how the rotor speed is evolving under the influence of applied torques and system dynamics.

Substituting $\dot{e_\omega} = \dot{\omega}_r^* - \dot{\omega}_r$ and the dynamics of $\dot{\omega}_r$:

$$\dot{e_\omega} = \dot{\omega}_r^* - \dot{\omega}_r = \dot{\omega}_r^* - \frac{1}{J}(T_e - T_l - B\omega_r) \quad (14)$$

Step 3: Design the Virtual Control Input

We design the control law for the electromagnetic torque generated by the motor T_e to stabilize the speed error e_ω. The reference torque is chosen as:

$$T_e = J(\dot{\omega}_r^* + k_p e_\omega + k_i\xi) + T_l + B\omega_r \quad (15)$$

where $k_p > 0$ is the proportional gain. Substituting T_e into the mechanical dynamics gives us the closed-loop system stability:

$$\dot{e_\omega} = \dot{\omega}_r^* - \frac{1}{J}\left(J(\dot{\omega}_r^* + k_p e_\omega + k_i\xi) + T_l + B\omega_r - T_l - B\omega_r\right)$$

$$\dot{e_\omega} = -k_p e_\omega - k_i\xi \quad (16)$$

Now substitute $\dot{e_\omega}$ into the expression for $\dot{V}_1$:

$$\dot{V}_1 = e_\omega(-k_p e_\omega - k_i\xi) + k_i\xi e_\omega$$

Simplifying this:

$$\dot{V}_1 = -k_p e_\omega^2 - k_i\xi e_\omega + k_i\xi e_\omega$$

$$\dot{V}_1 = -k_p e_\omega^2 \quad (17)$$

This expression shows that $\dot{V}_1 \leq 0$ because $k_p > 0$ and $e_\omega^2 \geq 0$. This implies that the Lyapunov function V_1 is non-increasing over time, meaning that the system's energy decreases or remains constant, but never increases. Since $\dot{V}_1 = 0$ only when $e_\omega = 0$, we can conclude that the error e_ω will eventually converge to zero, implying that the system achieves global asymptotic stability.

The inclusion of the integral term ξ in the Lyapunov function ensures that any steady-state error will also be eliminated. Even if there is a small error after transient responses, the integral action will continue accumulating the error over time, forcing it to zero.

Thus, the system is not only globally stable but also guarantees zero steady-state error in tracking the reference speed.

Step 4: Electromagnetic Torque Implementation

In a PMSM, the generated electromagnetic torque T_e is primarily controlled by the quadrature-axis current i_q, while the direct-axis current i_d is typically set to zero in surface-mounted PMSMs for optimal efficiency. The torque is related to i_q by using the torque equation (7). To derive the quadrature-axis current i_q^*, we first need to derive the control law for the required electromagnetic torque T_e. Using the backstepping control design approach, we specify the control law for the torque to stabilize the speed error. The torque command is designed as follows:

$$i_q^* = \frac{2}{3P\lambda_f}\left(J\left(\dot{\omega}_r^* + k_p e_\omega + k_i \xi\right) + T_l + B\omega_r\right) \quad (18)$$

This equation provides the desired reference current i_q^* in the q-axis, which is needed to generate the required torque T_e to drive the system to track the desired speed. where $J\left(\dot{\omega}_r^* + k_p e_\omega + k_i \xi\right)$ is the term that accounts for the system's inertia and provides the torque required to follow the reference speed. The proportional and integral gains ensure that both the current speed error and its accumulated history (integral of the error) are considered, T_l is load torque, if known or estimated, is included in the control law to compensate for external disturbances and $B\omega_r$ This term compensates for the friction in the motor, ensuring that the system responds appropriately in the presence of viscous damping.

Step 5: Extended Lyapunov Function (Control Design for Current Loops)

In backstepping control design, the Lyapunov function is a critical tool for proving the stability of the control system. For the current control loop of a PMSM, the Lyapunov function helps to ensure that the current errors converge to zero, leading to precise control of the motor currents. The second step in the backstepping control design for a PMSM involves stabilizing the current dynamics to ensure the desired electromagnetic torque is achieved. This step focuses on controlling the direct-axis (i_d) and quadrature-axis (i_q) current.

a. Define Current Errors

The desired i_d current, i_q is derived from the torque control law established in speed control section. For a surface-mounted PMSM, the direct-axis current i_d is typically regulated to zero for maximum torque per ampere (MTPA) control.

$$i_d^* = 0 \quad (19)$$

where i_d^* is typically zero for maximum torque per ampere control.

Define the current errors in the d-axis current as:

$$e_d = i_d - i_d^* \quad (20)$$

Define the current errors in the q-axis current as:

$$e_q = i_q - i_q^* \quad (21)$$

b. Design the Lyapunov Function for Current Control:

To achieve greater stabilization of the current dynamics, introduce an additional Lyapunov function that incorporates virtual control input. Extend this function to account for the current errors. Let i_q^* represent the desired q-axis current, and define the extended Lyapunov function V_2 as follows:

$$V_2 = V_1 + \frac{1}{2}e_d^2 + \frac{1}{2}e_q^2 \quad (22)$$

where $V_1 = \frac{1}{2}e_\omega^2 + \frac{1}{2}k_i\xi^2$, from the speed control loop, recall that: $\dot{V}_1 = -k_p e_\omega^2$. The time derivative of V_2 is:

$$\dot{V}_2 = \dot{V}_1 + e_d\dot{e}_d + e_q\dot{e}_q$$

$$\dot{V}_2 = -k_p e_\omega^2 + e_d\dot{e}_d + e_q\dot{e}_q \quad (23)$$

c. Electrical Dynamics of the PMSM

Using the current error dynamics for e_d and e_q:

$$\dot{e_d} = v_d - R_s i_d + \omega_r L_q i_q - L_d \dot{i_d} \quad (24)$$

$$\dot{e_q} = v_q - R_s i_q - \omega_r L_d i_d - \omega_r \lambda_f - L_q \dot{i_q} \quad (25)$$

d. Control Law for Stator Voltages

To ensure the stability of the current errors, design the control inputs, choose v_d, v_q to stabilize the currents based on the virtual control and system dynamics:

$$v_d = -k_d e_d + R_s i_d - \omega_r L_q i_q + L_d \dot{i_d} \quad (26)$$

$$v_q = -k_q e_q + R_s i_q + \omega_r L_d i_d + \omega_r \lambda_f + L_q \dot{i_q} \quad (27)$$

where k_d, k_q are positive control gains. Substitute these control laws into the derivatives of the current errors:

$$\dot{e_d} = R_s i_d - \omega_r L_q i_q - k_d e_d + L_d \dot{i_d} - R_s i_d + \omega_r L_q i_q - L_d \dot{i_d} \quad (28)$$

$$\dot{e_q} = R_s i_q + \omega_r L_d i_d + \omega_r \lambda_f - k_q e_q + L_q \dot{i_q} - R_s i_q - \omega_r L_d i_d - \omega_r \lambda_f - L_q \dot{i_q} \quad (29)$$

e. Current Error Dynamics:

The current error dynamics ensure that the d-axis (e_d) and q-axis (e_q) current errors converge to zero through properly designed control laws.

$$\dot{e_d} = -k_d e_d \quad (30)$$

$$\dot{e_q} = -k_q e_q \quad (31)$$

Substitute the expressions for $\dot{e_d}$ and $\dot{e_q}$ into the derivative of the Lyapunov function:

$$\dot{V}_2 = -k_p e_\omega^2 + e_d(-k_d e_d) + e_q\left(-k_q e_q\right) \quad (32)$$

Simplify:

$$\dot{V}_2 = -k_p e_\omega^2 - k_d e_d^2 - k_q e_q^2 \quad (33)$$

Research Article | Volume 13, Issue 1 | Pages 69-79 | e-ISSN: 2347-470X

This equation shows that the derivative of the Lyapunov function is a negative quadratic form, which is essential for proving stability.

Step 6: Stability Proof: Global Asymptotic Stability

To prove the stability of the system, we analyze $\dot{V}_2$ as follows:

a. Non-positive

From the equation (33), since all gains $k_p > 0$, $k_d > 0$, and $k_q > 0$ are positive constants, and $e_\omega^2 \geq 0$, $e_d^2 \geq 0$, and $e_q^2 \geq 0$ for all time, we can conclude that:

$$\dot{V}_2 \leq 0 \qquad (34)$$

This implies that the Lyapunov function V_2 is non-increasing over time, meaning that the system's energy is either decreasing or staying constant, but never increasing. The fact that $\dot{V}_2 \leq 0$ guarantees that the system will not diverge and that the errors will not grow.

b. Energy Dissipation

The terms $-k_p e_\omega^2, -k_d e_d^2$, and $-k_q e_q^2$ represent the rate at which the system dissipates energy associated with the speed and current errors. As the energy is dissipated, the system approaches a state where these errors go to zero.

- $e_\omega \to 0$: The rotor speed will converge to the desired reference speed.
- $e_d \to 0$: The *d*-axis current will converge to the desired reference value (typically zero for maximum torque per ampere in surface-mounted PMSMs).
- $e_q \to 0$: The *q*-axis current will converge to the reference value i_q^*, which generates the necessary torque.

c. Convergence to Zero

The quadratic form $-k_p e_\omega^2 - k_d e_d^2 - k_q e_q^2$ ensures that the Lyapunov function $\dot{V}_2$ is strictly negative unless all the errors are zero:

$$\dot{V}_2 = 0 \text{ if and only if } e_\omega = 0,\ e_d = 0,\ e_q = 0$$

This condition implies that the system can only reach a steady state when the speed error e_ω, the *d*-axis current error e_d, and the *q*-axis current error e_q all converge to zero. In other words, the system reaches its equilibrium state only when the desired rotor speed and current values are perfectly tracked.

d. Global Asymptotic Stability

The fact that $\dot{V}_2 \leq 0$ and $\dot{V}_2 = 0$ only when $e_\omega = 0$, $e_d = 0$, and $e_q = 0$ proves that the system is globally asymptotically stable. This means that, regardless of the initial conditions (i.e., the starting values of e_ω, e_d, and e_q), the system will eventually settle into a stable state where all errors are zero.

4. SIMULATION RESULTS AND DISCUSSIONS

4.1 Development of Simulation Model for PMSM Speed Control

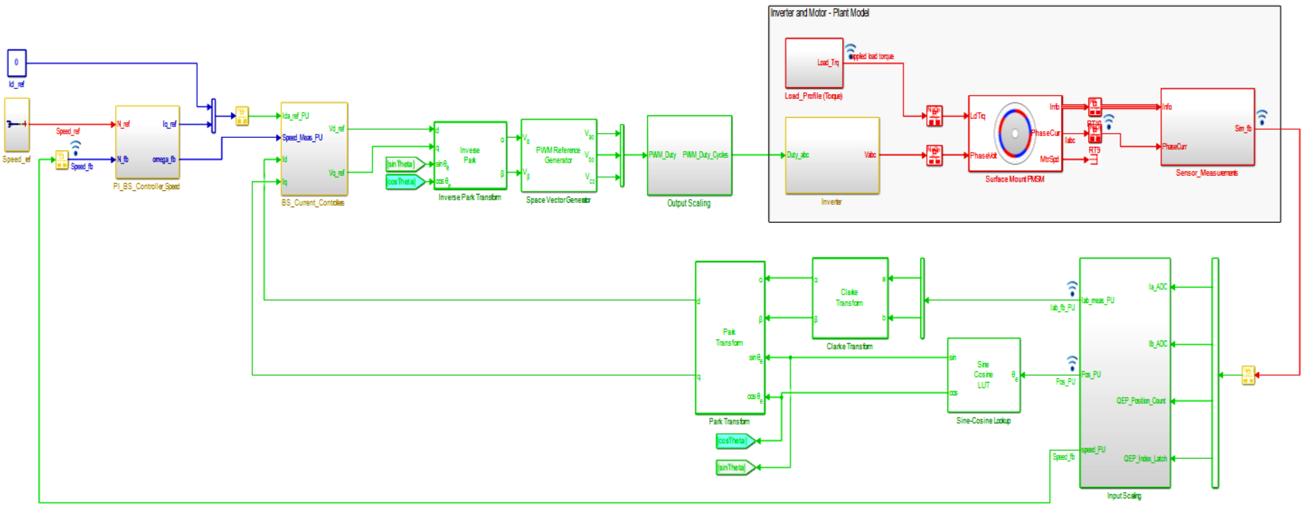

Figure 1. Simulation model for PMSM speed control using PI Backstepping Controllers

A robust and detailed simulation model is vital for validating the effectiveness of the Backstepping Controller in achieving precise speed control under varying operational conditions. Illustrated in *figure 2*, this model includes key components controller, inverter, motor, and transformations integrated within Simulink's modular framework. This modular approach allows for a realistic and adaptable environment to rigorously evaluate the proposed backstepping-based control method, demonstrating its capability for accurate speed tracking and robust performance across different scenarios. The proposed control strategy for speed control of a Permanent Magnet Synchronous Motor (PMSM) was developed and implemented in MATLAB Simulink, utilizing the Motor Control Blockset. This simulation model is based on a Teknic M-2310P-LN-04K

FOREX Publication
Open Access | Rapid and quality publishing

International Journal of
Electrical and Electronics Research (IJEER)
Research Article | Volume 13, Issue 1 | Pages 69-79 | e-ISSN: 2347-470X

PMSM motor, a BOOSTXL-DRV8305EVM, and a TI F28379D LaunchPad, ensuring an accurate representation of real-world components. The Surface-Mounted PMSM parameters are detailed in *table 1*, the PI gain-scheduling configurations in *table 2*, and the PI Backstepping Control Gains in *table 3*.

Table 1. PMSM Parameters

Parameters	Values
DC-Link voltage [V]	24
Pole pairs number	4
Stator Resistor per phase [Ω]	0.36
D-axis inductance [H]	2.0000e-04
Q-axis inductance [H]	2.0000e-04
Inertia [kg/m^2]	7.0616e-06
Friction Co-efficient [kg-m^2/s]	2.6369e-06
Permanent magnet flux [Wb]	0.0063954
Continuous Torque [Nm]	0.2724
Rated Speed [RPM]	4000

Table 2. GSPI Gain Controller

GSPI speed control gain	k_p	k_i
operating speed points 0.2	0.2600	3.6264
operating speed points 0.9	0.2748	0.0840
load torque applied	3.4165	37.7240
operating speed points -0.8	0.2251	0.0920
Current Controller		
PI *d*-axis current control gain	3.0929	5634.3
PI *q*-axis current control gain	3.0929	5634.3

Table 3. Backstepping Gain Controller

PI-BS Gain Controller	
$k_{p\omega}$	6783
$k_{i\omega}$	1485800
k_d	2.997
k_q	3.7597

4.2. Simulation Results for Backstepping Control Performance

To evaluate the effectiveness of the proposed PI Backstepping (PI-BS) controller, its performance is benchmarked against the Gain-Scheduled PI (GSPI) control method presented in the previous work, "Speed Control of Surface-Mounted PMSM Using the Gain-Schedule PI Control Method" [9]. The GSPI method is a widely used approach for handling the nonlinear dynamics of Surface-Mounted Permanent Magnet Synchronous Motors (SM-PMSMs) by dynamically adjusting the PI controller gains based on operating conditions. While effective in steady-state conditions, the GSPI method has demonstrated limitations in transient response, disturbance rejection, and handling rapid speed transitions. These challenges highlight the need for more robust control strategies, motivating the development of the PI-BS controller. By addressing these limitations through Lyapunov-based stability analysis and integral action in the speed control loop, the PI-BS controller aims to achieve superior performance in both transient and steady-state scenarios. The subsequent simulation results provide a detailed comparison between the two methods under identical test conditions, including step changes, nonlinear load disturbances, and speed reversals, to demonstrate the advantages of the PI-BS controller. These scenarios involve a series of step changes in the reference speed, starting with the motor stationary at 0 RPM, stepping up to 821.4 RPM (0.2 PU) at 0 seconds, and subsequently to 3,696.3 RPM (0.9 PU) at 0.5 seconds. At 1.0 seconds, a nonlinear load torque is applied to evaluate disturbance rejection, followed by a final step change to -3,285.6 RPM (-0.8 PU) at 1.5 seconds to test the controller's performance during rapid deceleration and speed reversal.

figure 3 provides a detailed analysis of the motor speed response for a Permanent Magnet Synchronous Motor (PMSM) under step reference inputs and nonlinear load disturbances, comparing the performance of the Gain-Scheduled PI (GSPI) and PI Backstepping (PI-BS) controllers. The presented results emphasize the effectiveness of the PI-BS controller in managing dynamic transitions, disturbances, and speed reversals with enhanced stability and precision.

In *figure 3(a)*, the general motor speed response illustrates the system's behavior under step changes at 0.5 seconds and 1.5 seconds. The PI-BS controller demonstrates smoother and more stable transitions compared to the GSPI controller. While both controllers track the reference speed, the PI-BS controller exhibits faster stabilization and reduced oscillations, highlighting its robustness in handling dynamic scenarios and external disturbances.

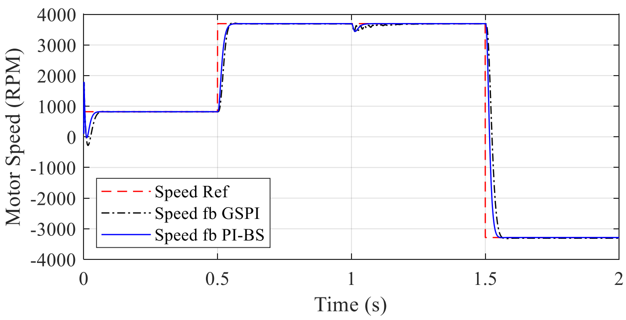

(a)

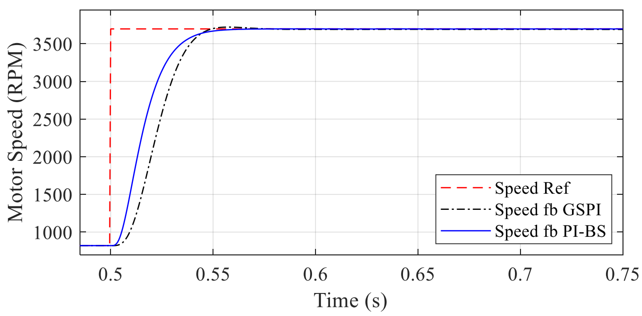

(b)

FOREX Publication
Open Access | Rapid and quality publishing
International Journal of
Electrical and Electronics Research (IJEER)
Research Article | Volume 13, Issue 1 | Pages 69-79 | e-ISSN: 2347-470X

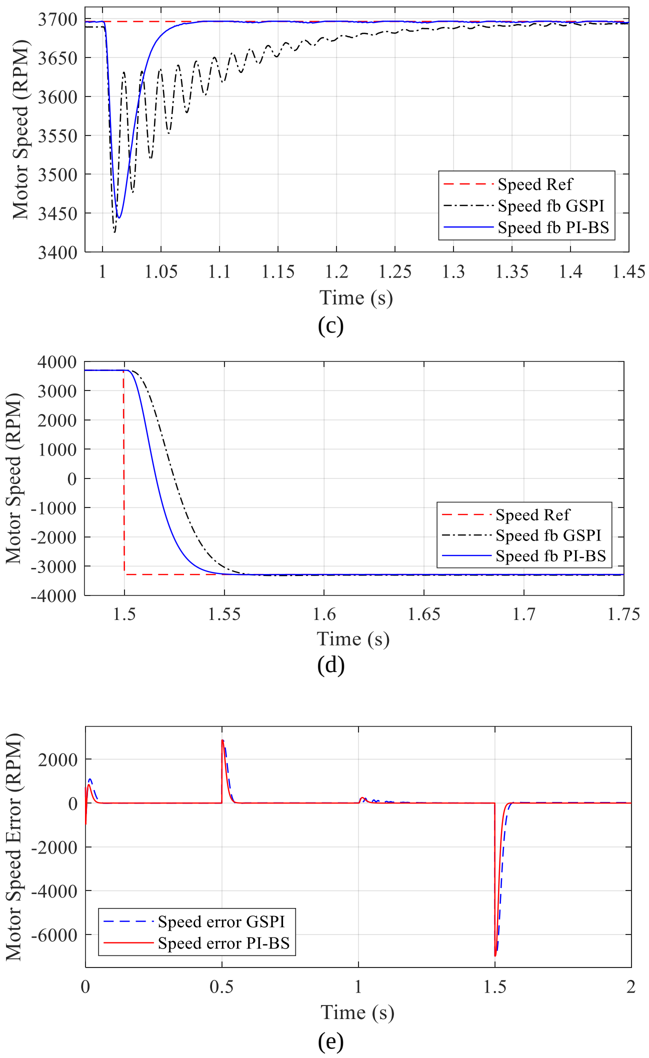

Figure 3. Simulation results compare the motor speed (RPM) response of a Permanent Magnet Synchronous Motor under step reference inputs. (a) Motor Speed Response for PMSM under Reference Step Inputs and Nonlinear Load Torque; (b) Zoomed View of Motor Speed Response around 0.5 Seconds; (c) Zoomed View of Motor Speed Response around 1.0 Second; (d) Zoomed view around the 1.5 second; (e) Comparison of Motor Speed Error for GSPI and PI-BS Controllers over the Full Simulation Period.

The transient performance around 0.5 seconds, shown in *Figure 3(b)*, quantifies the superiority of the PI-BS controller with a rise time of 19.26 ms and an overshoot of 0.50%, compared to the GSPI controller's rise time of 22.83 ms and overshoot of 1.53%. These results underline the PI-BS controller's faster and more accurate response, ensuring minimal deviation from the desired reference speed during step changes.

At 1.0 second, when a nonlinear load torque disturbance is applied, *figure 3(c)* shows that the PI-BS controller efficiently suppresses oscillations and quickly stabilizes the motor speed. In contrast, the GSPI controller struggles with pronounced oscillations, demonstrating the PI-BS controller's superior disturbance rejection capability. Similarly, during the speed reversal at 1.5 seconds, as seen in *figure 3(d)*, the PI-BS controller achieves a fall time of 17.92 ms with minimal overshoot (0.50%), outperforming the GSPI controller's slower fall time of 28.04 ms and higher overshoot of 1.82%.

figure 3(e) provides a comprehensive comparison of motor speed error between the Gain-Scheduled PI (GSPI) controller and the PI Backstepping (PI-BS) controller over the full simulation period. Speed error is defined as the difference between the reference speed and the actual motor speed. Across the simulation, the PI-BS controller consistently exhibits lower speed errors, particularly during key transitions and disturbances. For instance, during the step change at 0.5 seconds to 3,696.3 RPM, the PI-BS controller demonstrates a smaller peak error and quicker response compared to the GSPI controller, which experiences more significant deviations and takes longer to settle. Similarly, during the major speed reversal at 1.5 seconds to -3,285.6 RPM, the PI-BS controller again shows a smoother and faster response, with significantly less overshoot and quicker convergence to the desired speed, resulting in smaller speed errors compared to the GSPI controller, which struggles with pronounced oscillations. When a nonlinear load torque is applied at 1.0 seconds, the PI-BS controller exhibits superior disturbance rejection, rapidly correcting the speed error, whereas the GSPI controller experiences prolonged oscillations and slower recovery. Overall, the PI Backstepping Controller outperforms the GSPI controller, maintaining better accuracy, faster response times, and more effective disturbance rejection, resulting in consistently lower speed errors throughout the simulation. This figure highlights the robustness and precision of the PI Backstepping Control strategy in dynamic PMSM applications, particularly under challenging operating conditions.

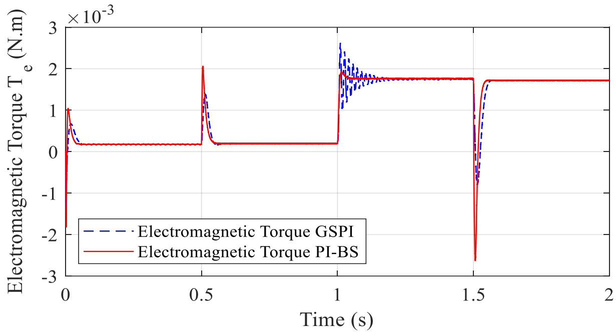

Figure 4. Electromagnetic Torque Response for GSPI and PI-BS Controllers

figure 4 compares the electromagnetic torque T_e responses of the Gain-Scheduled PI (GSPI) and PI Backstepping (PI-BS) controllers over the simulation period. The PI-BS controller (red solid line) consistently delivers smoother transitions, faster stabilization, and fewer oscillations than the GSPI controller (blue dashed line). At 0.5 seconds, during a step change to 0.9 PU (3,696.3 RPM), the PI-BS controller demonstrates steady torque adjustment with minimal overshoot, while the GSPI controller experiences pronounced oscillations. Similarly, at 1.0 seconds, when a nonlinear load torque is applied, the GSPI controller struggles with high-frequency oscillations, whereas the PI-BS controller quickly restores stability. During the sharp speed reversal to -0.8 PU (−3,285.6 RPM) at 1.5 seconds, the PI-BS controller maintains smooth torque output, contrasting

FOREX Publication
Open Access | Rapid and quality publishing
International Journal of
Electrical and Electronics Research (IJEER)
Research Article | Volume 13, Issue 1 | Pages 69-79 | e-ISSN: 2347-470X

with the GSPI controller's slower recovery and significant oscillations. These results highlight the PI-BS controller's superior torque regulation, ensuring reliable motor performance under large speed transitions and external disturbances.

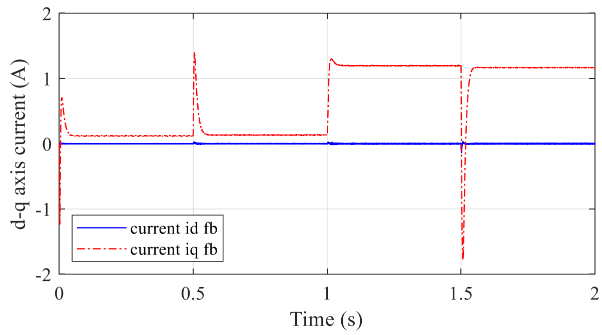

Figure 5. d-q axis current

figure 5 illustrates the d-axis (i_d) and q-axis (i_q) current feedback over the simulation period. The blue solid line represents i_d, regulated near zero to maximize torque efficiency in surface-mounted PMSM control by adhering to the Maximum Torque Per Ampere (MTPA) strategy. This confirms the objective of minimizing d-axis current to reduce losses and enhance q-axis current utilization for torque production. The red dashed line shows i_q, which closely tracks the required reference during speed transitions. At 0.5 seconds, 1.0 seconds (nonlinear load torque application), and 1.5 seconds (speed reversal to -0.8 PU), i_q exhibits sharp adjustments, particularly at 1.5 seconds, where a speed reversal causes a distinct spike before stabilization. These responses highlight the controller's robustness in dynamically adjusting i_q to meet torque demands while maintaining i_d near zero, ensuring efficient and reliable performance under varying operating conditions.

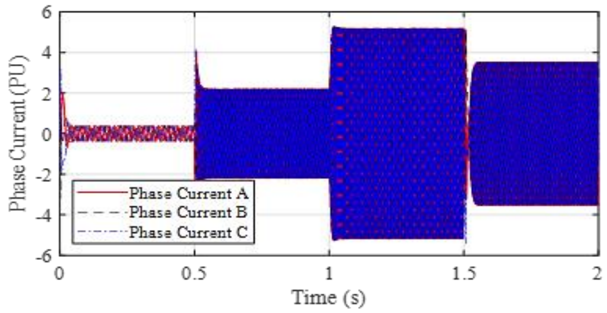

(a)

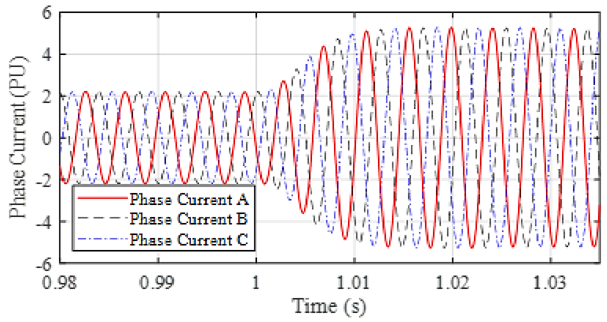

(b)

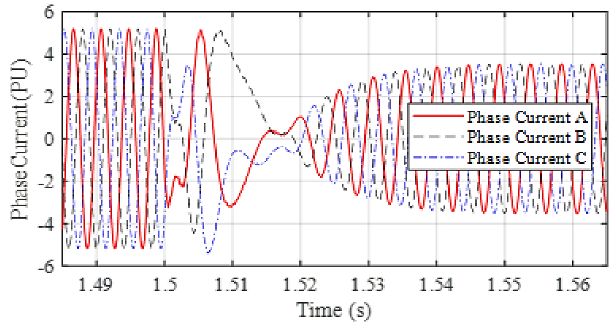

(c)

Figure 6. Stator currents of phases A, B and C. (a) Overall Phase Current Response; (b) Zoomed View at 1.0 Seconds; (c) Zoomed View at 1.5 Seconds.

figure 6 illustrates the stator currents of phases A, B, and C during the simulation period, with specific zoomed views highlighting dynamic responses at critical transitions. The currents are expressed in per unit (PU), with Phase A represented by the red solid line, Phase B by the black dashed line, and Phase C by the blue dotted line. These currents are essential for generating the electromagnetic torque needed for motor speed regulation. *figure 6(a)* shows the full simulation period, where step changes in current magnitude occur at 0.5 seconds, 1.0 seconds (nonlinear load torque application), and 1.5 seconds (speed reversal). The three-phase currents exhibit a balanced sinusoidal pattern in steady-state, ensuring efficient motor operation. During transitions, the current amplitudes dynamically adjust to meet new torque demands, reflecting the controller's ability to manage torque generation effectively. *figure 6(b)* provides a zoomed view around 1.0 seconds, capturing the system's response to the application of a nonlinear load torque. The phase currents display increased oscillatory behavior, reflecting the motor's effort to compensate for the disturbance. These oscillations gradually subside, demonstrating the system's capability to restore stability after external torque variations. *figure 6(c)* focuses on the sharp speed reversal at 1.5 seconds. The phase currents undergo a noticeable phase and amplitude shift, adapting to the rapid change in motor speed. Although transient oscillations are observed immediately following the reversal, the system successfully stabilizes the phase currents, restoring a sinusoidal pattern with minimal delay.

These results confirm the critical role of phase currents in adapting to dynamic operating conditions. The balanced sinusoidal pattern in steady-state conditions highlights the system's efficiency, while the controlled response to transient oscillations demonstrates the robustness of the controller in maintaining torque and speed stability under varying loads and speed transitions.

5. CONCLUSION

The PI Backstepping (PI-BS) Controller has proven to be a highly effective and robust control strategy for the speed regulation of Permanent Magnet Synchronous Motors (PMSMs), offering significant improvements in dynamic performance, stability, and disturbance rejection. Extensive simulation results across various scenarios consistently demonstrate the PI-BS controller's superiority over conventional methods, such as the Gain-Scheduled PI (GSPI) controller. Notably, in Figure 3(b), during the step change from 0.2 PU to 0.9 PU, the PI-BS controller achieves a faster rise time of 19.26ms and minimal overshoot of 0.50%, compared to the GSPI controller's rise time of 22.83ms and overshoot of 1.53%, highlighting the PI-BS controller's quicker and more accurate response. Similarly, *figure 3(c)* demonstrates the PI-BS controller's superior ability to reject disturbances during the application of a nonlinear load torque at 1.0 second, where the PI-BS controller recovers faster with significantly fewer oscillations than the GSPI controller, underscoring its robustness in handling external perturbations. Additionally, in Figure 3(d), during the rapid deceleration and speed reversal from 0.9 PU to -0.8 PU, the PI-BS controller achieves a fall time of 17.92ms and an overshoot of 0.50%, far outperforming the GSPI controller's fall time of 28.04ms and overshoot of 1.82%. These results highlight the PI-BS controller's capability to manage rapid speed transitions, maintain motor stability under nonlinear disturbances, and achieve precise torque regulation through efficient q-axis current control while minimizing d-axis current for maximum efficiency. The controller's faster response times, reduced overshoot, and improved disturbance rejection make it a more advanced and reliable solution for high-performance motor control applications. The PI Backstepping Controller's exceptional ability to handle dynamic transitions and external disturbances makes it an ideal choice for demanding applications where motor performance, efficiency, and reliability are critical. This makes it particularly well-suited for industrial automation, automotive systems, and other high-performance environments that require precise control and robust operation.

REFERENCES

[1] O. E. Özçiflikçi, M. Koç, S. Bahçeci, and S. Emiroğlu, "Overview of PMSM control strategies in electric vehicles: a review," Int J Dyn Control, vol. 12, no. 6, pp. 2093–2107, Jun. 2024, doi: 10.1007/s40435-023-01314-2.

[2] W.-S. Jung, H.-K. Lee, Y.-K. Lee, S.-M. Kim, J.-I. Lee, and J.-Y. Choi, "Analysis and Comparison of Permanent Magnet Synchronous Motors According to Rotor Type under the Same Design Specifications," Energies (Basel), vol. 16, no. 3, p. 1306, Jan. 2023, doi: 10.3390/en16031306.

[3] H. Wang, G. Zhang, and X. Liu, "Speed Control for PMSM with Fast-Terminal Super-Twisting Sliding Mode Controller via Extended State Disturbance Observer," Applied Sciences, vol. 14, no. 18, p. 8126, Sep. 2024, doi: 10.3390/app14188126.

[4] F. Mohd Zaihidee, S. Mekhilef, and M. Mubin, "Robust Speed Control of PMSM Using Sliding Mode Control (SMC)—A Review," Energies (Basel), vol. 12, no. 9, p. 1669, May 2019, doi: 10.3390/en12091669.

[5] R. I. Sudjoko, Hartono, and P. Iswahyudi, "Speed Control of Permanent Magnet Synchronous Motor Using Universal Bridge and PID Controller," 2020, pp. 405–416. doi: 10.1007/978-981-15-4481-1_39.

[6] S. Mandava and V. R. Nippatla, "Speed and current feedback loops control for permanent magnet synchronous motor using PID controller," 2024, p. 040013. doi: 10.1063/5.0189794.

[7] M. H. Mousavi, M. E. Karami, M. Ahmadi, P. Sharafi, and F. Veysi, "Robust speed controller design for permanent magnet synchronous motor based on gain-scheduled control method via LMI approach," SN Appl Sci, vol. 2, no. 10, Oct. 2020, doi: 10.1007/s42452-020-03453-z.

[8] Y. Lee, S. H. Lee, and C. C. Chung, "LPV H∞ Control with Disturbance Estimation for Permanent Magnet Synchronous Motors," IEEE Transactions on Industrial Electronics, vol. 65, no. 1, pp. 488–497, Jan. 2018, doi: 10.1109/TIE.2017.2721911.

[9] S. Nhek, S. Srang, C. Srun, S. Seven, R. Mao, and S. Chann, "Speed Control of Surface-Mounted PMSM Using the Gain-Schedule PI Control Method," in 2024 7th International Conference on Green Technology and Sustainable Development (GTSD), Ho Chi Minh City, Vietnam: IEEE, Jul. 2024, pp. 62–66. doi: 10.1109/GTSD62346.2024.10674748.

[10] F. A. Samman, C. Srun, and R. S. Sadjad, "Adaptive look-up table and interpolated PI gain scheduling control for voltage regulator using DC-DC converter," International Journal of Innovative Computing, Information and Control, vol. 15, no. 2, pp. 489–501, Apr. 2019, doi: 10.24507/ijicic.15.02.489.

[11] M. M. Alshbib, M. M. Elgbaily, I. M. Alsofyani, and F. Anayi, "Performance Enhancement of Direct Torque and Rotor Flux Control (DTRFC) of a Three-Phase Induction Motor over the Entire Speed Range: Experimental Validation," Machines, vol. 11, no. 1, p. 22, Dec. 2022, doi: 10.3390/machines11010022.

[12] M. Alshbib and S. Abdulkerim, "An Experimental and Analytical Investigation of the Direct Torque Control Method of a Three-Phase Induction Motor," Journal of Electrical Engineering & Technology, vol. 18, no. 6, pp. 4367–4379, Nov. 2023, doi: 10.1007/s42835-023-01483-2.

[13] F. Yang et al., "Improved direct torque control strategy for reducing torque ripple in switched reluctance motors," Journal of Power Electronics, vol. 22, no. 4, pp. 603–613, Apr. 2022, doi: 10.1007/s43236-021-00380-z.

[14] A. Nasr, C. Gu, X. Wang, G. Buticchi, S. Bozhko, and C. Gerada, "Torque-Performance Improvement for Direct Torque-Controlled PMSM Drives Based on Duty-Ratio Regulation," IEEE Trans Power Electron, vol. 37, no. 1, pp. 749–760, Jan. 2022, doi: 10.1109/TPEL.2021.3093344.

[15] A. K. Sahoo and R. K. Jena, "Reduction of torque ripple in induction motor-driven electric vehicle using optimized stator flux," International Journal of Information Technology, vol. 15, no. 3, pp. 1333–1346, Mar. 2023, doi: 10.1007/s41870-023-01172-3.

[16] A. Najem, A. Moutabir, A. Ouchatti, and M. El Haissouf, "Experimental Validation of the Generation of Direct and Quadratic Reference Currents by Combining the Ant Colony Optimization Algorithm and Sliding Mode Control in PMSM using the Process PIL," International Journal of Robotics and Control Systems, vol. 4, no. 1, pp. 188–216, 2024, doi: 10.31763/ijrcs.v4i1.1286.

[17] J. Yang, Z. Zhou, and J. Ji, "Nonlinear Integral Sliding Mode Control with Adaptive Extreme Learning Machine and Robust Control Term for Anti-External Disturbance Robotic Manipulator," Arab J Sci Eng, vol. 48, no. 2, pp. 2375–2397, Feb. 2023, doi: 10.1007/s13369-022-07246-x.

[18] H. Alnami, C. Pang, and Q. Wang, "A Novel Sliding Mode Control Method of Interior-Mounted PMSM," in 2021 IEEE Texas Power and Energy Conference (TPEC), IEEE, Feb. 2021, pp. 1–6. doi: 10.1109/TPEC51183.2021.9384961.

[19] A. Wang and S. Wei, "Sliding Mode Control for Permanent Magnet Synchronous Motor Drive Based on an Improved Exponential Reaching Law," IEEE Access, vol. 7, pp. 146866–146875, 2019, doi: 10.1109/ACCESS.2019.2946349.

[20] J. Michalski, M. Mrotek, M. Retinger, and P. Kozierski, "Adaptive Active Disturbance Rejection Control with Recursive Parameter

International Journal of
Electrical and Electronics Research (IJEER)
Research Article | Volume 13, Issue 1 | Pages 69-79 | e-ISSN: 2347-470X

Identification," Electronics (Basel), vol. 13, no. 16, p. 3114, Aug. 2024, doi: 10.3390/electronics13163114.

[21] Q. Zheng and Z. Gao, "Active disturbance rejection control: some recent experimental and industrial case studies," Control Theory and Technology, vol. 16, no. 4, pp. 301–313, Nov. 2018, doi: 10.1007/s11768-018-8142-x.

[22] X. Zhang, Y. Chen, and X. Sun, "Overview of Active Disturbance Rejection Control for Permanent Magnet Synchronous Motors," Journal of Electrical Engineering & Technology, vol. 19, no. 3, pp. 1237–1255, Mar. 2024, doi: 10.1007/s42835-023-01710-w.

[23] S. Shi, Z. Zeng, C. Zhao, L. Guo, and P. Chen, "Improved Active Disturbance Rejection Control (ADRC) with Extended State Filters," Energies (Basel), vol. 15, no. 16, p. 5799, Aug. 2022, doi: 10.3390/en15165799.

[24] Y. Lee, S.-H. Lee, and C. C. Chung, "LPV H∞ Control with Disturbance Estimation for Permanent Magnet Synchronous Motors," IEEE Transactions on Industrial Electronics, vol. 65, no. 1, pp. 488–497, Jan. 2018, doi: 10.1109/TIE.2017.2721911.

[25] Runze Cai, Ruixiang Zheng, Ming Liu, and Mian Li, "Robust control of PMSM using geometric model reduction and μ-synthesis," in IECON 2016 - 42nd Annual Conference of the IEEE Industrial Electronics Society, IEEE, Oct. 2016, pp. 2885–2891. doi: 10.1109/IECON.2016.7793602.

[26] S. Muthurajan, R. Loganathan, and R. R. Hemamalini, "Deep Reinforcement Learning Algorithm based PMSM Motor Control for Energy Management of Hybrid Electric Vehicles," WSEAS TRANSACTIONS ON POWER SYSTEMS, vol. 18, pp. 18–25, Mar. 2023, doi: 10.37394/232016.2023.18.3.

[27] Z. Song, J. Yang, X. Mei, T. Tao, and M. Xu, "Deep reinforcement learning for permanent magnet synchronous motor speed control systems," Neural Comput Appl, vol. 33, no. 10, pp. 5409–5418, May 2021, doi: 10.1007/s00521-020-05352-1.

[28] H. Echeikh, R. Trabelsi, A. Iqbal, N. Bianchi, and M. F. Mimouni, "Comparative study between the rotor flux-oriented control and non-linear backstepping control of a five-phase induction motor drive – an experimental validation," IET Power Electronics, vol. 9, no. 13, pp. 2510–2521, Oct. 2016, doi: 10.1049/iet-pel.2015.0726.

[29] M. Elmahfoud, B. Bossoufi, M. Taoussi, N. El Ouanjli, and A. Derouich, "Comparative Study Between Backstepping Adaptive and Field Oriented Controls for Doubly Fed Induction Motor," European Journal of Electrical Engineering, vol. 22, no. 3, pp. 209–221, Jun. 2020, doi: 10.18280/ejee.220302.

[30] A. Senhaji, M. Abdelouhab, A. Attar, and J. Bouchnaif, "Backstepping control of a permanent magnet synchronous motor," Mater Today Proc, vol. 72, pp. 3730–3737, 2023, doi: 10.1016/j.matpr.2022.09.248.

[31] M. Zamani, N. van de Wouw, and R. Majumdar, "Backstepping controller synthesis and characterizations of incremental stability," Syst Control Lett, vol. 62, no. 10, pp. 949–962, Oct. 2013, doi: 10.1016/j.sysconle.2013.07.002.